MULTIPHYSICS MODELING OF ADVECTION-DOMINATED TWO-PHASE COMPOSITIONAL FLOW IN POROUS MEDIA

JOCHEN FRITZ, BERND FLEMISCH, RAINER HELMIG

Abstract. A new multiphysics model for two-phase compositional flow is presented. It is designed to fit the level of model complexity to that of the flow and transport processes taking place in a given region of the domain. Thus, the model domain is divided into a subdomain which accounts for two-phase compositonal processes and another in which single-phase transport is described. A coupling of the simple and complex equations gives rise to an efficient model. Special interest is placed in the discretization of the two-phase compositional model in a finite-volume context and an IMPES time scheme with decoupled pressure and transport equations. For optimal subdomain determination, an easy-to-handle, adaptive scheme is presented. The practical usability is demonstrated on a real live problem from carbon dioxide sequestration.

Key words: multiphysics, domain decomposition, multiphase flow, compositional, sequential, decoupled formulation

1. Introduction. The modeling of flow processes in porous media is used in many environmental and engineering applications. To gain insight to increasingly complex processes, models in use become increasingly complex which has obvious consequences for the computational effort. When considering large systems, detailed measurements (such as saturations of contaminants or concentrations of certain components) are usually only available in relatively small regions in which complex processes are assumed to occur, whereas fewer and simpler measurements may be available in other parts of the considered domain. This poor spatial resolution of measurement data in large parts of the model domain questions the use of highly complex and detailed models. More important, complex processesoften occur only in a small part of the domain of interest. in order to account for these factors, the coupling of a two-phase compositional model to a single-phase transport model is presented. This allows for the use of the complex two-phase compositional model only in the parts of the model domain where complex processes occur, whereas other parts of the domain are resolved by a simpler single-phase model.

Coupling of different models for the simulation of complex processes was for example originally discussed in the context of domain decomposition methods (e.g., [12]). This was the motivation for [18], where the authors develop a multiblock framework to couple fully implicit and sequential two-phase flow models. Further developments resulted in multiphysics coupling of single-phase (implicit or sequential), two-phase (implicit or sequential) and black-oil (implicit only) models as published in [19] and [17]. However, the coupling of the different models involved a nonlinear iterative solver to match the coupling conditions at the interfaces. Furthermore, the black-oil model was only presented in a fully implicit formulation which in turn involves nonlinear solvers. Due to the relatively simple form of the pressure equations, the resulting smaller matrices and the noniterative solution sceme, sequential models require less computational effort per timestep, making them attractive in wide areas of application ([4]). The black-oil model also contains rather strong assumptions (water phase contains no other components than water, gas phase is only made up of light hydrocarbons), limiting its applicability to certain areas.

To account for the mentioned data collection problem, a multi-scale multi-physics model approach was presented in [16]. In this study, the velocity is assumed to be divergence-free. This assumption, however, is not true for compositional multi-phase flow, since the mixing of phases influences the total fluid volume.

We introduce a sequential multiphysics model for two-phase compositional flow whithout the need for nonlinear solvers and without restrictions concerning miscibility. For this purpose, we incorporate the decoupled formulation for two-phase compositional flow introduced and analyzed in [21] and expanded to other formulations of the pressure equation in [7]. We want to concentrate on applications like enhanced recovery of contaminated soils or carbon dioxide sequestration, where we assume strongly advection-dominated problems and hence neglect diffusion and capillarity.

2. Physical Model.

2.1. General balance equation. The mass balance equation per component in a multiphase compositional model neglecting diffusion is (e.g., [13])

$$\frac{\partial C^\kappa}{\partial t} = -\nabla \cdot \sum_\alpha \mathbf{v}_\alpha \varrho_\alpha X_\alpha^\kappa + q^\kappa \,, \tag{2.1}$$

where $C^\kappa = \phi \sum_\alpha S_\alpha \varrho_\alpha X_\alpha^\kappa$ denotes the total concentration of component κ, and ϕ is the porosity. Moreover, S_α and ϱ_α are the saturation and the density of phase α, respectively, while X_α^κ is the mass fraction of component κ in phase α. The source term of component κ in the unit mass per time is denoted by q^κ. Given the mobility $\lambda_\alpha = \frac{k_{r\alpha}}{\mu_\alpha}$ – where μ_α and $k_{r\alpha}$ are the dynamic viscosity and the relative permeability of phase α, respectively– , the pressure p, the permeability tensor $\mathbf{K}$ and the gravity vector $\mathbf{g}$, the velocity of phase α is given by the extended Darcy law as

$$\mathbf{v}_\alpha = \lambda_\alpha \mathbf{K} \nabla \left(p - \varrho_\alpha \mathbf{g} \right) \,. \tag{2.2}$$

2.2. Pressure equation. As a physical constraint, the pore space of the porous medium must always be filled with a mixture of fluids. That is, the sum over the volumes of the phases inside a control volume must equal the pore volume, or

$$\left(\sum_\kappa C^\kappa \right) \cdot \left(\sum_\alpha \frac{\nu_\alpha}{\varrho_\alpha} \right) - \phi = 0 \,, \tag{2.3}$$

where $\nu_\alpha = \frac{S_\alpha \varrho_\alpha}{\sum_\alpha S_\alpha \varrho_\alpha}$ denotes the mass fraction of phase α. Due to compressibilities and mixing effects, the volume of a mixture is affected by changes in pressure or total concentration. These volume changes must be taken into account in the pressure equation to conserve the total volume of the mixture at any point in space. Following [7] or [14], the pressure equation is expressed by

$$-\frac{\partial v_t}{\partial p}\frac{\partial p}{\partial t} + \sum_\kappa \frac{\partial v_t}{\partial C^\kappa} \nabla \cdot \sum_\alpha X_\alpha^\kappa \varrho_\alpha \mathbf{v}_\alpha = \sum_\kappa \frac{\partial v_t}{\partial C^\kappa} q^\kappa \,, \tag{2.4}$$

where v_t is the total specific volume of the mixture. The final pressure euqation is then obtained by inserting Darcy's law (2.2) into equation (2.4). The unit of the terms of equation (2.4) is volume per time, thus it is essentially a volume conservation equation. The equation predicts changes in total fluid volume caused by changes in concentration of the components and compensates them by adjusting the pressure field accordingly. Since the first-order approximation of the volume changes in equation (2.4) is not perfect yet, volumetric errors may still occur. Therefore we follow the suggestion in [21], where the authors add the residual of the volume constraint (2.3) to the right-hand side of equation (2.4) to compensate these errors in subsequent time steps.

2.3. Flash calculation. The pressure and transport equations are evaluated sequentially in every time step. Since the transport equations (2.1) can only evaluate changes in total concentration, the saturation and mass fractions have to be evaluated by a flash calculation at the end of every time step. In [1], the authors present a detailed description of flash calculations for arbitrary numbers of phases and components. Without going into detail on the derivation, the set of $n_\alpha - 1$ (n_α is the number of phases) equations

$$\sum_\kappa \frac{z^\kappa \left(K_\alpha^\kappa - 1\right)}{1 + \sum\limits_{\alpha \neq r} \left(K_\alpha^\kappa - 1\right) \nu_\alpha} = 0 \, \forall \alpha \neq r \,, \tag{2.5}$$

known as the Rachford-Rice equation has to be solved iteratively in order to determine the mass fraction of each phase ν_α. In this equation, $z^\kappa = \frac{C^\kappa}{\sum\limits_\kappa C^\kappa}$ denotes the overall mass fraction of component κ in the mixture, whereas the equilibrium ratio K_α^κ relates the mass fraction of component κ in phase α to its mass fraction in a reference phase r through $K_\alpha^\kappa = \frac{X_\alpha^\kappa}{X_r^\kappa}$. A fast and adequately exact way to obtain the equilibrium ratios is the exploitation of Dalton's, Raoult's, and Henry's laws as presented in [16]. In this case, the equilibrium ratios stay constant for the isothermal model. A more accurate way is to incorporate thermodynamic equations of state (EOS) and calculate the equilibrium ratios from the component's fugacities in the different phases, as described in [1] or [15]. In this case, the equilibrium ratios are subject to the phase compositions and, therefore, have to be updated in every iteration step. For simplicity, however, we use the former approach. The mass fractions of the components in the reference phase can be calculated from

$$X_r^\kappa = \frac{z^\kappa}{\sum\limits_{\alpha \neq r} \left(K_\alpha^\kappa - 1\right) \nu_\alpha + 1} \,, \tag{2.6}$$

while the mass fractions in the other phases can be obtained by rearranging the definition of the equilibrium ratios to

$$X_\alpha^\kappa = K_\alpha^\kappa X_r^\alpha \,. \tag{2.7}$$

For a two-phase two-component system with the phases $\alpha = w$, n and the reference phase being w, the Rachford-Rice equation reduces to

$$\nu_n = \frac{z^1 \left(K_n^1 - 1\right) + z^2 \left(K_n^2 - 1\right)}{\left(K_n^1 - 1\right) \cdot \left(K_n^2 - 1\right)} \,, \tag{2.8}$$

which can be directly solved. For a stable two-phase system, the phase mass fraction ν_n must have a value between zero and unity: $0 < \nu_n < 1$. Inserting these two inequalities into equation (2.8) yields the stability constraints (e.g., [20]) for a two-phase system

$$\begin{aligned} \sum_\kappa K_n^\kappa z^\kappa > 1 \,, \\ \sum_\kappa \frac{K_n^\kappa}{z^\kappa} > 1 \,. \end{aligned} \tag{2.9}$$

If one of these constraints is violated, the mixture is in a single-phase state. Violation of the former constraint corresponds to a single wetting phase w, violation of the latter to a single nonwetting phase n. In these cases, the composition of the remaining phase equals the feed mass fractions $X_\alpha^\kappa = z^\kappa$.

2.4. Single-phase transport. The pressure and transport equations for incompressible single-phase transport can be derived as simplifications from equations (2.1) and (2.4). By inserting the definition of the total concentration into the mass balance equation (2.1) for one phase and applying the chain rule, we get

$$\phi\varrho_\alpha X_\alpha^\kappa \frac{\partial S_\alpha}{\partial t} + S\varrho_\alpha X_\alpha^\kappa \frac{\partial \phi}{\partial t} + \phi S_\alpha X_\alpha^\kappa \frac{\partial \varrho_\alpha}{\partial t} + \phi S_\alpha \varrho_\alpha \frac{\partial X_\alpha^\kappa}{\partial t} = -\varrho_\alpha \nabla \cdot (\mathbf{v}_\alpha X_\alpha^\kappa) + q^\kappa \,. \tag{2.10}$$

Since only one phase is present, the saturation equals unity and hence the derivative of saturation in the first term on the left-hand side equals zero. For incompressible flow, the derivatives of density and porosity also vanish. We now assume a volumetric source term Q of the present phase with a defined mass fraction X_Q^κ. Then the mass source of component κ is $q^\kappa = \varrho Q X_Q^\kappa$, and we can write the transport equation as

$$\phi \frac{\partial X^\kappa}{\partial t} = -\nabla \cdot (\mathbf{v} X) + Q X_Q^\kappa \,, \tag{2.11}$$

where we neglected the indicces of the remaining phase for better readability. Obviously, the mass fraction of the source must be defined in such a way, that the flow from the source does not split in two phases. This transport equation must only be solved for one component in the binary system since mass fractions sum up to unity. The pressure equation can also be simplified for an incompressible single-phase system by deleting the first term on the left hand side and setting the remaining volume derivative $\frac{\partial v_t}{\partial C^\kappa}$ to the reciprocal of the density ϱ of the present phase:

$$\frac{1}{\varrho} \nabla \cdot \sum_\kappa X^\kappa \varrho \mathbf{v} = \sum_\kappa \frac{1}{\varrho} q^\kappa \tag{2.12}$$

Once again using the chain rule and the fact that mass fractions sum up to unity, and using the source term as defined above, we get the pressure equation for single-phase flow,

$$\nabla \cdot \mathbf{v} = Q \,. \tag{2.13}$$

Our simple model of incompressible single-phase transport is thus described by equations (2.11) and (2.13) combined with Darcy's law (2.2).

2.5. Multiphysics. A comparison of the two pressure equations (2.4) and (2.13) reveals their resemblance: just as described above for equation (2.4), the terms of equation (2.13) have the unit volume per time. Their common physical relevance is the conservation of the total fluid volume at any point in space. Also, the transport equations can be derived from each other and represent the conservation of mass. This basically opens the way for our multiphysics approach where the model domain is divided into two parts: one subdomain of special interest which is modeled with higher physical accuracy and the global domain where reasonable simplifications can be made. As an example, consider figure 2.1 where a model problem, as it commonly appears in environmental sciences, is sketched. The domain is filled with water except

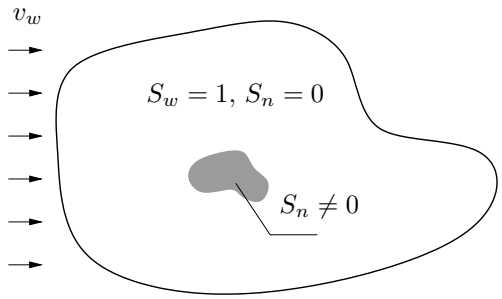

FIG. 2.1. *Multiphysics problem example*

at a spill of non aqueous phase liquid (NAPL) containing contaminants. The contaminants are dissolved in water and transported by the water flow. At the same time, the NAPL spill is displaced. Due to the solution of contaminants in water, this scenario would have to be simulated using a two-phase compositional model. However, this model is only needed in the area where the NAPL spill is situated. The rest of the domain can be modeled using a single-phase transport model. Coupling these two models leads to our multiphysics approach. By exploiting the similarities of the pressure equations and writing both of them into the same stiffnes matrix as described in section 3.3, there is no need for further coupling conditions and corresponding special solution schemes.

3. Numerical Model. The discretization of the equations described above is realized using a standard cell-centered finite volume method (FVM) and an IMPES time discretization. These are implemented in the toolbox DuMu$^{\mathrm{X}}$([11]) which was build on the numerical environment DUNE ([2, 3]). In every timestep, the pressure equation is solved implicitly using the coefficient values of the old time level and, thereafter, the transport equation is solved explicitly. The solution of the transport equations of single-phase and multiphase compositional models and the pressure equation of single-phase models have been discussed by many authors, as for example in [8]. We want to concentrate on our solution strategy for the compositional pressure equation (2.4).

3.1. Discretization of the pressure equation. For the discretization of partial differential equations by the FVM, the model domain is divided into control volumes and the equation is integrated over each control volume G. The integration of equation (2.4) over G and the use of the Gauss-Green formula yields

$$\begin{aligned} -\frac{\partial V_t}{\partial p}\frac{\partial p}{\partial t} + \oint \mathbf{n} \cdot \sum_\alpha \left(\mathbf{v}_\alpha \varrho_\alpha \sum_\kappa \frac{\partial v_t}{\partial C^\kappa} X_\alpha^\kappa \right) d\Gamma \\ + \int \sum_\kappa \left(\nabla \frac{\partial v_t}{\partial C^\kappa} \cdot \sum_\alpha X_\alpha^\kappa \varrho_\alpha \mathbf{v}_\alpha \right) dG = |V| \sum_\kappa \frac{\partial v_t}{\partial C^\kappa} q^\kappa \,, \end{aligned} \tag{3.1}$$

where Γ denotes the boundary of G. The integral of the total fluid volume $\int v_t dG$ is denoted by V_t. In the right hand side term, the source is assumed to be piecewise constant so its integral equals its multiplication by the control volume$|V|$. Inserting

equation (2.2) and separating pressure gradients and gravity vectors , one gets

$$
\begin{aligned}
&-\frac{\partial V_t}{\partial p}\frac{\partial p}{\partial t} - \oint \mathbf{n}\left[(\mathbf{K}\nabla p)\sum_\alpha\left(\lambda_\alpha \varrho_\alpha \sum_\kappa \frac{\partial v_t}{\partial C^\kappa} X_\alpha^\kappa\right)\right] d\Gamma \\
&- \int (\mathbf{K}\nabla p)\sum_\kappa\left(\nabla\frac{\partial v_t}{\partial C^\kappa}\sum_\alpha X_\alpha^\kappa \varrho_\alpha\lambda_\alpha\right) dG \\
&= -\oint \mathbf{n}\cdot\left[(\mathbf{Kg})\sum_\alpha\left(\lambda_\alpha\varrho_\alpha\sum_\kappa\frac{\partial v_t}{\partial C^\kappa}X_\alpha^\kappa\right)\right] d\Gamma \\
&- \int (\mathbf{Kg})\sum_\kappa\left(\nabla\frac{\partial v_t}{\partial C^\kappa}\sum_\alpha X_\alpha^\kappa\varrho_\alpha\lambda_\alpha\right) dG + |V|\sum_\kappa\frac{\partial v_t}{\partial C^\kappa}q^\kappa\,. \qquad (3.2)
\end{aligned}
$$

$\oint \mathbf{n}\cdot$ is discretized as $\sum_k |A_k|\,\mathbf{n}_k\cdot$, where k is the index for the cell interfaces as sketched on the left-hand side of figure (3.1), and $|A_k|$ is the area of the cell face k, the pressure gradient ∇p is discretized by $-\frac{p-p_k}{|\mathbf{u_k}|}\frac{\mathbf{u_k}}{|\mathbf{u_k}|}$, where p is the pressure in the current cell and p_k is the pressure in the k-th neighbor cell, while $\mathbf{u}_k$ is the vector conneting the two centers of gravity. The gradient of the volume derivative $\nabla\frac{\partial v_t}{\partial C^\kappa}$ is discretized in the same way as the pressure gradient. By a decomposition of the control volume as sketched in figure (3.1), the computation of the volume integrals in the second and fourth term of equation (3.2) can be carried out by using the standard face gradients of pressure and volume derivative. In particular, each interface k is assigned a weighting factor w_k to decompose the control volume to a subvolume $w_k\cdot|V|$ (see figure (3.1), right-hand side). Obviously the weighting factors must sum to unity. For the integration, the coefficients inside the integral are evaluated at the interface and multiplied with the associated subvolume. The discretized form of equation (3.2) is then

$$
\begin{aligned}
&-\frac{\partial V_t}{\partial p}\cdot\frac{p^{t-\Delta t}-p^t}{\Delta t} \\
&+\sum_k |A_k|\,\mathbf{n}_k\cdot\mathbf{K}\frac{\mathbf{u}_k}{|\mathbf{u}_k|}\frac{p^t-p_k^t}{|\mathbf{u}_k|}\sum_\alpha\left(\lambda_\alpha\varrho_\alpha\sum_\kappa\frac{\partial v_t}{\partial C^\kappa}X_\alpha^\kappa\right) \\
&+\sum_k |V|\,w_k\frac{p^t-p_k^t}{|\mathbf{u}_k|}\mathbf{K}\frac{\mathbf{u}_k}{|\mathbf{u}_k|}\cdot\sum_\kappa\left(-\frac{\frac{\partial v_t}{\partial C^\kappa}-\left(\frac{\partial v_t}{\partial C^\kappa}\right)_k}{|\mathbf{u_k}|}\frac{\mathbf{u_k}}{|\mathbf{u_k}|}\sum_\alpha X_\alpha^\kappa\varrho_\alpha\lambda_\alpha\right) \\
&= |V|\sum\frac{\partial v_t}{\partial C^\kappa}\cdot q^\kappa \\
&-\sum_k |A_k|\,\mathbf{n}_k\cdot\mathbf{Kg}\sum_\alpha\left(\lambda_\alpha\varrho_\alpha\sum_\kappa\frac{\partial v_t}{\partial C^\kappa}X_\alpha^\kappa\right) \\
&-\sum_k |V|\,w_k\mathbf{Kg}\cdot\sum_\kappa\left(-\frac{\frac{\partial v_t}{\partial C^\kappa}-\left(\frac{\partial v_t}{\partial C^\kappa}\right)_k}{|\mathbf{u_k}|}\frac{\mathbf{u_k}}{|\mathbf{u_k}|}\sum_\alpha X_\alpha^\kappa\varrho_\alpha\lambda_\alpha\right)\,. \qquad (3.3)
\end{aligned}
$$

Pressures marked with the superscript t are the unknowns and those with the superscript $t-\Delta t$ are taken from the last time step as all other coefficients. Equation (3.3) has to be set up for every control volume and forms a linear system of equations which can be solved explicitly for the pressures p^t. It turnes out that the discussed volume integral in the second and fourth term of equation (3.2) and their discretized

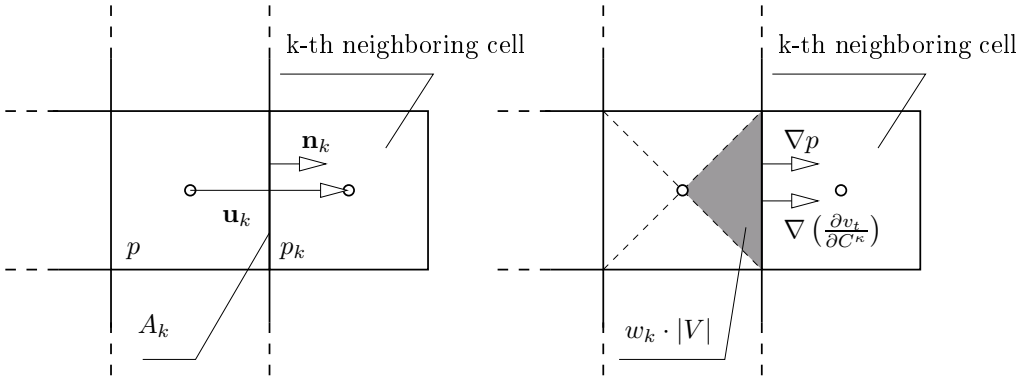

FIG. 3.1. *Vector and interface notation in FVM scheme*

version in equation (3.3), respectively, do not lead to significant improvements of the gained solution and may as well be neglected. They may, however, have stabilizing effects in some setups.

The evaluation of coefficients at the cell interfaces is done by full upwinding. The only exceptions are the volume derivatives which are always taken from the current cell. The upwind cell is determined by evaluating each total phase potential

$$\Phi_\alpha = p + \varrho_\alpha \mathbf{g} \,.$$

At this point, special care must be taken for gravity-dominated systems where countercurrent flow may occur since upwind directions can be different for different phases. For the upwinding of coefficients during the setup of the pressure equation, the pressures of the last time step are used. Thus, an initial guess of the value of pressure is necessary for te first timestep. Also for the initialization of saturations and mass fractions, an initial pressure guess is necessary. We use a standard two-phase fractional flow pressure equation with centrally weighted total mobilities (e.g., [6] or [13]) to obtain such a guess.

3.2. Evaluation of volume derivatives:. The volume derivatives $\frac{\partial v_t}{\partial C^\kappa}$ are calculated numerically with a secant method (e.g., [5]): In a pre-step, the transport equation is evaluated with the last timestep's pressure field to determine increments. The current phase split (or phase mass fraction) ν_α is known from the last flash calculation or by calculating

$$\nu_\alpha = \frac{S_\alpha \cdot \varrho_\alpha}{\sum\limits_\alpha S_\alpha \cdot \varrho_\alpha} \,.$$

The current total fluid volume is then determined by

$$v_{t,curr} = \sum_\alpha \nu_\alpha \cdot \frac{1}{\varrho_\alpha} \,.$$

Now, the total concentration of the first component is increased by the increment i^κ which was calculated in the pre-step, and a flash calculation is performed. With the mass fractions X_α^κ and the phase splits ν_α, the total fluid volume $v_{t,incr.\kappa}$ with respect

to the increased total concentration can be computed. The derivative can now easily be found

$$\frac{\partial v_t}{\partial C^\kappa} = \frac{v_{t,incr.\kappa} - v_{t,curr}}{i^\kappa} .$$

This procedure is repeated for each component.

3.3. Multiphysics. As already mentioned earlier, the pressure equations of the two-phase compositional and the single-phase transport model have the same physical relevancet, the same dimensions and the same unknowns. Exploiting this similarity, the two sets of equations are used in one system of equations. The entries of the stiffness matrix are set according to the position of the corresponding control volume inside the domain. If the control volume is situated inside the subdomain for the two-phase compositional model, the matrix and right-hand side entry is set according to equation (3.3). If the control volume lies outside of the subdomain, the entries are set according to the discretized form of equation (2.13). This strategy can be applied properly also for control volumes adjacent to the subdomain boundary since all necessary coefficients can be determined: for the second phase, they only have to be set to zero outside the subdomain, and hence the corresponding terms in the two-phase compositional pressure equation vanish. The only constraint is that only the phase which is present outside the subdomain can flow across the boundary. The same considerations as for the pressure equations are valid for the transport equations: all necessary coefficients can be determined by setting them to zero for the second phase outside the subdomain, and thus all terms related to this phase vanish.

3.4. Choice and adaption of the subdomain. For the proposed multiphysics model, the choice of an adequate sub-domain is crucial for the quality of the result. The above mentioned constraint, that only one phase may flow across the subdomain boundary has to be fulfilled. Furthermore, demixing effects have to be respected. Consider for example a domain filled with water and residually saturated gas with a pressure-driven water flux. The gas dissolves in water and gets transported further. The solubility of air in water is proportional to pressure and since pressure decreases downstream exsolution of gas occurs, producing very small saturations of non-mobile air. If the solubility is exceeded outside the subdomain, the demixing effect can not be reproduced since no flash calculations are carried out in the single-phase transport model. Exsolution of gas occurs predominantly in cells adjacent to the two-phase region. That is because the water which comes from the upstream cell is fully saturated with gas, and the pressure is slightly smaller in the downstream cell. The most logical choice of the subdomain therefore contains all control volumes where two phases are present and – to avoid superfluous velocity calculations – all adjacent cells. At the end of each timestep, the cells inside the subdomain are checked: if two phases are present, the cell remains in the subdomain and also all neighbors become part of the subdomain. Furthermore, the mass fractions of the cells outside the subdomain can be compared to the solubility of the dissolved component. This quite easy decomposition can only be expected to be sucesful in the case of an explicit solution of the transport equations. In particular, the fulfilment of the CFL-condition guarantees that no modeling error will occur, since information is transported at most one cell further in one timestep.

4. Examples. We demonstrate the performance of our approach with two examples. The dynamic adaptivity of the subdomain is shown on a two-dimensional exam-

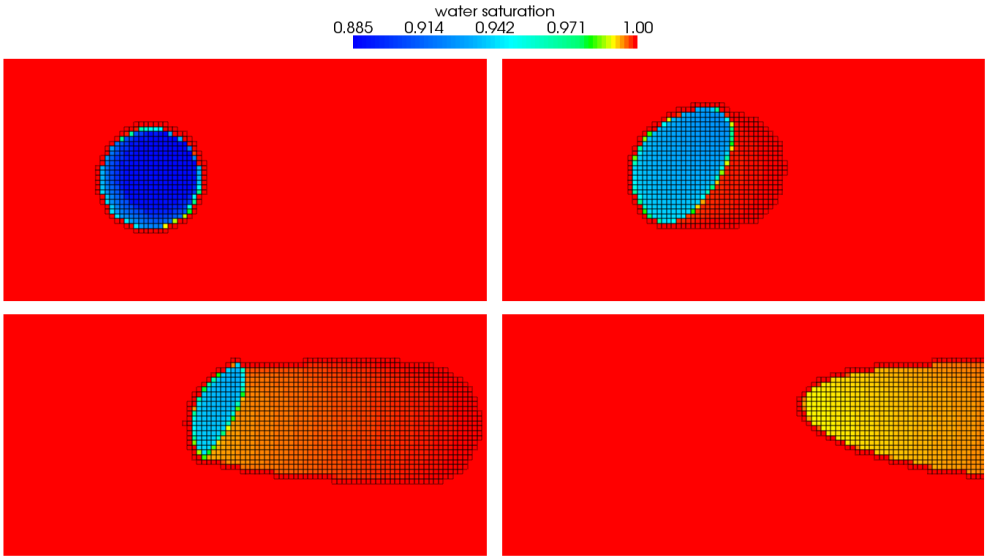

FIG. 4.1. *Example for dynamic subdomain adaptivity. From upper left to lower right, the system is shown for initial conditions and after 100, 200 and 300 timesteps, respectively. The subdomain is marked by black squares.*

ple, whereas the applicability to real-life problems is demonstrated on the Johannsen-formation benchmark from carbon dioxide sequestration.

4.1. Subdomain adaptivity. To demonstrate the subdomain adaptivity we set up a simple example in a rectangular domain with no-flow boundaries at the top and bottom and hydrostatic pressure boundaries at the left and right. The domain is initially filled with water, except for a given region where air is found in a low saturation. The water saturation at the left boundary equals unity, and on the right there is a free-flow boundary. The pressure at the left boundary is higher than at the right and thus a pressure- and gravity-driven flow is induced. Several processes occur at the same time: 1) the air moves up and to the right, 2) in the two-phase region, air is dissolved in water, 3) exsolution occurs further downstream. Figure 4.1 shows the system at initial conditions and after 100, 200 and 300 timesteps, respectively. Saturation of water is displayed according to the legend, and the subdomain is marked by black squares. During the first 100 timesteps, the air moves advectively until the residual saturation of 0.05 is reached. Dissolution and exsolution produce a plume of air with very low saturation. The subdomain grows to cover the two-phase region. At some point, cells which do not contain gas any more, are no longer covered by the subdomain as can be seen after 200 timesteps on the lower left of figure 4.1. Finally, when most of the air has dissolved, the subdomain becomes smaller again and moves downsteam as shown on the lower right.

4.2. Carbon dioxide sequestration benchmark. In [10], a benchmark problem treating the injection of carbon dioxide through a single well into a deep aquifer is presented (see also [9]). The given grid is made up of 54756 control volumes. We chose this benchmark to compare the performance of the two-phase compositional model and the multiphysics model with a realistic problem. Both methods solved the given problems with 9540 time steps for the first 25 years of injection. Figure

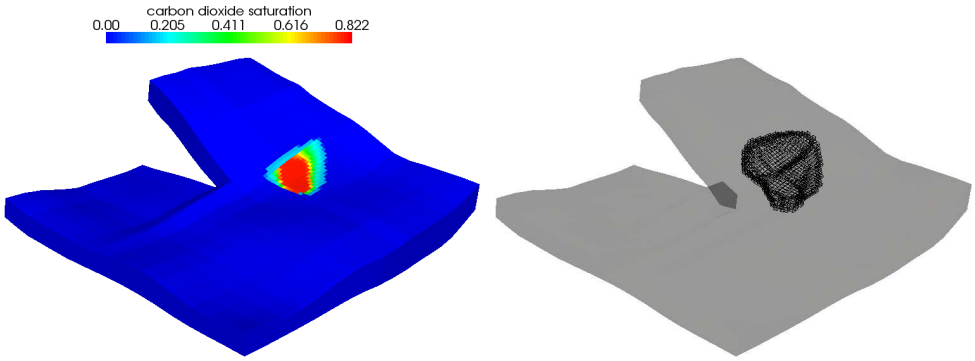

FIG. 4.2. *Results for the Johannsen formation benchmark after 25 years and corresponding subdomain*

4.2 shows the resulting saturation of carbon dioxide in the reservoir on the left-hand side and the subdomain, which occupies 2355 cells (4.3 % of the total domain) in the last timestep, on the right-hand side. In this example, the multiphysics model provided a speed up of 21 % compared to the full compositional model. The number of calls of the flash calculation in the full compositional model was 22 times as high as in the multiphysics model. In our example we used simple relations to determine equilibrium ratios (see section 2.3) and a noniterative flash, making the evaluation of the flash calculation only marginally relevant for the overall computational costs. However, according to [20], for equation of state simulators, 70 % of the CPU time is spent on flash calculation, making the use of a multiphysics model, and hence the reduction of flash-calculation calls, highly attractive.

5. Conclusions . We presented a multiphysics method which is able to couple two-phase compositional flow and single-phase transport models. The requirement for the presented method is the concentration of two-phase flow in subdomains and presence of only one phase in the rest of the domain. The model helps to minimize superfluous evaluations of material laws, which results in savings of computational costs and data. In particular, the potential increase in efficiency is influenced by sizes of regions where two-phase flow and mass transfer processes occur, and the complexity of physical relations being used especially in the two-phase region. Using a simple adaptive scheme, the subdomain size can be readjusted constantly during the simulation to obtain an efficient discretization and simultaneously guarantee exact results. However, further developments concerning diffusion and capillary effects must be made in order to make the method usable for a wide ranges of application. This may make the solution of the transport equation problematic, since explicit Euler (and also Runge-Kutta) timestepping schemes can only deal with hyperbolic equations. Although Peclet numbers of $Pe = 500$ did not seem to compromise the stability of the model in [14], simulation scenarios in which the influence of diffusion or capillary effects is high, will require operator splitting or other appropriate schemes.

6. Acknowledgment. We thank Bradley Mallison from Stanford University for his help with the compositional model.

Authors are members of the International Research Training Group NUPUS, financed by the German Research Foundation (DFG) and The Netherlands Organisation for Scientific Research (NWO), and thank the DFG (GRK 1398) and NWO (DN 81-754) for their support.

REFERENCES

[1] K. Aziz and T.W. Wong. Considerations in the development of multipurpose reservoir simulation models. In *Proceedings First and Second International Forum on Reservoir Simulation*, pages 77–208. Steiner, P., 1989.

[2] P. Bastian, M. Blatt, A. Dedner, C. Engwer, R. Klöfkorn, M. Ohlberger, and O. Sander. A generic grid interface for parallel and adaptive scientific computing. part i: Abstract framework. *Computing*, 82(2-3):103–119, 2008.

[3] P. Bastian, M. Blatt, A. Dedner, C. Engwer, R. Klöfkorn, M. Ohlberger, and O. Sander. A generic grid interface for parallel and adaptive scientific computing. part ii: Implementation and tests in dune. *Computing*, 82(2-3):121–183, 2008.

[4] P. Binning and M.A. Celia. Practical implementation of the fractional flow approach to multiphase flow simulation. *Advances in Water Resources*, 22(5):461–478, 1999.

[5] I.N. Bronstein and K.A. Semendjajew. *Handbook of Mathematics*. Springer; 3rd edition, 1997.

[6] Y. Cao, B. Eikemo, and R. Helmig. Fractional flow formulation for two-phase flow in porous media. *http://www.nupus.uni-stuttgart.de/media/publications/NUPUS_2007-01_online.pdf*, 2007.

[7] Z. Chen, Q. Guan, and R.E. Ewing. Analysis of a compositional model for fluid flow in porous media. *SIAM Journal on Applied Mathematics*, 60(3):747–777, 2000.

[8] Z. Chen, G. Huan, and Y. Ma. *Computational Methods for Multiphase Flows in Porous Media*. SIAM, 2006.

[9] H. Class, H. Dahle, F. Riis, A. Ebigbo, and G. Eigestad. Numerical investigations of co2 sequestration in geological formations: Problem-oriented benchmarks problem 3: Estimation of the co2 storage capacity of a geological formation. *http://www.hydrosys.uni-stuttgart.de/co2-workshop/correctedProblem3.pdf*, 2007.

[10] G.T. Eigestad, H.K. Dahle, B. Hellevang, W.T. Johansen, F. Riis, and E. Øian. Geological modeling and simulation of co2 injection in the johansen formation. *Computational Geosciences*, submitted.

[11] B. Flemisch, J. Fritz, R. Helmig, J. Niessner, and B. Wohlmuth. Dumux: A multi-scale multiphysics toolbox for flow and transport processes in porous media. In *Multi-scale Computational Methods for Solids and Fluids*, pages 69–74. European Community on Computational Methods in Applied Sciences, 2007.

[12] R. Glowinski and M.F. Wheeler. Domain decomposition and mixed finite element methods for elliptic problems. In *Domain Decomposition methods for Partial Differential Equations*, pages 144–172. SIAM, 1988.

[13] R. Helmig. *Multiphase Flow and Transport Processes in the Subsurface*. Springer, 1997.

[14] K. Jessen, M.G. Gerritsen, and B.T. Mallison. High-resolution prediction of enhanced condensate recovery processes. *SPE 99619*, 2006.

[15] L.X. Nghiem and Y.-K. Li. Computation of multiphase equilibrium phenomena with an equation of state. *Fluid Phase Equilibria*, 17(1):77–95, 1984.

[16] J. Niessner and R Helmig. Multi-scale modeling of three-phase–three-component processes in heterogeneous porous media. *Advances in Water Resources*, 30(11):2309–2325, 2007.

[17] M. Peszynska. Multiphysics coupling for two phase flow in degenerate conditions. In J. Chadam, A. Cunningham, R.E. Ewing, P. Ortoleva, and M.F. Wheeler, editors, *Resource Recovery, Confinement, and Remediation of Environmental Hazards*. Springer, 2002.

[18] M. Peszynska, Q. Lu, and M.F. Wheeler. Coupling different numerical algorithms for two phase fluid flow. In J.R. Whiteman, editor, *The Mathematics of Finite Elements and Applications X*, pages 205–214. Elsevier, 1999.

[19] M. Peszynska, Q. Lu, and M.F. Wheeler. Multiphysics coupling of codes. In *Computational Methods in Water Resources*, pages 175–182. A. A. Balkema, 2000.

[20] E.H. Stenby and P. Wang. Noniterative phase equilibrium calculation in compositional reservoir simulation. *SPE 26641*, 1993.

[21] J.A. Trangenstein and J.B. Bell. Mathematical structure of compositional reservoir simulation.

SIAM J. Sci. Stat. Comput., 10(5):817–845, 1989.